

# Dynamical correlations and domain wall relocation in transverse field Ising chains

Philippe Suchsland,<sup>1</sup> Benoît Douçot,<sup>1,2</sup> Vedika Khemani,<sup>3</sup> and Roderich Moessner<sup>1</sup>

<sup>1</sup>Max Planck Institute for the Physics of Complex Systems, Nöthnitzer Str. 38, 01187 Dresden, Germany

<sup>2</sup>LPTHE, UMR 7589, CNRS and Sorbonne Université, 75252 Paris Cedex 05, France

<sup>3</sup>Department of Physics, Stanford University, Stanford, California 94305, USA

We study order parameters and out-of-time-ordered correlators (OTOCs) for a wide variety of transverse field Ising chains: classical and quantum, clean and disordered, integrable and generic. The setting we consider is that of a quantum quench. We find a remarkably rich phenomenology, ranging from stable periodic to signals decaying with varying rates. This variety is due to a complex interplay of dynamical constraints (imposed by integrability and symmetry) which thermalisation is subject to. In particular, a process we term dynamical domain wall relocation provides a long-lived signal in the clean, integrable case, which can be degraded by the addition of disorder even without interactions. Our results shed light on a proposal to use an OTOC specifically as a local dynamical diagnostic of a quantum phase transition even when evaluated in a state with an energy density corresponding to the paramagnetic phase.

*Introduction.*—The advent of experiments on coherently evolving quantum matter has led to an interdisciplinary focus on quantum dynamics [1–17]. In contrast to conventional time-ordered dynamical correlation functions,  $\langle O_p(t)O_m \rangle$ , several recent studies have focused on out-of-time-ordered correlators (OTOCs),  $\langle O_p(t)O_m O_p(t)O_m \rangle$ . First proposed by Larkin et al. [18–28], OTOCs probe how a system retains or loses memory of its initial state when subject to a perturbation, and have been studied in relation to a variety of phenomena ranging from quantum chaos to black hole physics to operator spreading and information scrambling [29–35].

One recent line of enquiry concerns the possible capacity of OTOCs to diagnose quantum phase transitions in quench experiments from excited states in a way which is not accessible to traditional time-ordered correlators [36–42]. A case in point is the quantum phase transition in the one dimensional transverse field Ising model (TFIM), where recent work provided numerical evidence that the non-vanishing OTOC of an order parameter (concretely, the local magnetization) evaluated at late times detects presence of ground state ordering *even starting from an initially fully polarised state* [36, 37, 41, 42]. The numerics indicated this behavior for both the TFIM, which is integrable, and a perturbed non-integrable model with interactions. These results were surprising because the polarized state is a finite temperature state for any non-zero transverse field, and clean one dimensional systems do not order at finite temperature [43]. Indeed, in contrast to the OTOC, standard temporal correlators of the magnetization decay to zero, as expected from thermalization to a paramagnetic finite temperature equilibrium state. This raises the theoretical question of how the OTOC might manage to evade thermalization so as to detect the order present in the ground state of the Hamiltonian, but absent in equilibrium at the energy density corresponding to the initial state of the quench.

Our work provides a detailed study of OTOCs across a variety of Ising chains, with a particular focus on using OTOCs as diagnostics of quantum phase transitions. We first study the integrable  $S = 1/2$  TFIM, and pro-

vide an explicit computation of the OTOC starting from the fully polarized state. We show that this does indeed have a non-zero asymptote everywhere in the ferromagnetic phase, even as the time-ordered autocorrelator of the magnetization vanishes. We uncover a strikingly rich phenomenology in this model (Table I), which we account for in detail via a formulation in terms of pairing wavefunctions à la BCS. We identify the physical processes underpinning the dynamics of domain walls, a central one being their dynamical relocation, which is linked to both the absence of chaos and explains the numerically observed signal in the OTOC. We further find that the state underpinning the OTOC signal resembles a rotated state with low entanglement.

These twin observations, in turn, motivate the study of an analogous classical Ising chain. Here we find that *both* the OTOC and the autocorrelator of the magnetization exhibit a non-vanishing late-time signal, which is a consequence of a failure of the magnetization to thermalize fully. Indeed, by adding a small amount of disorder to the couplings, keeping an ordered ground state while removing translational invariance of the Hamiltonian (but not the initial state), thermalization, and hence vanishing, of the magnetisation does set in classically. Analogously, the OTOC in the quantum setting is degraded by disorder.

This in turn suggests that the non-vanishing late-time OTOC in this set-up is predicated on the non-ergodicity arising from the integrability of the TFIM. Indeed, a perturbed non-integrable Ising magnet, initialised with a fully polarised state at weak transverse field, is doubly proximate to integrability. First, on account of the weakness of the perturbation; second, as a result of hosting a small density of – and hence weakly interacting – domain walls. The apparently non-vanishing OTOC thus is likely only a prethermal signal, visible on the short-to-intermediate times to which present-day numerical tools are limited.

In the following, we introduce the model, notation and dynamical observables. We then give a detailed overview of the phenomenology found for the OTOC

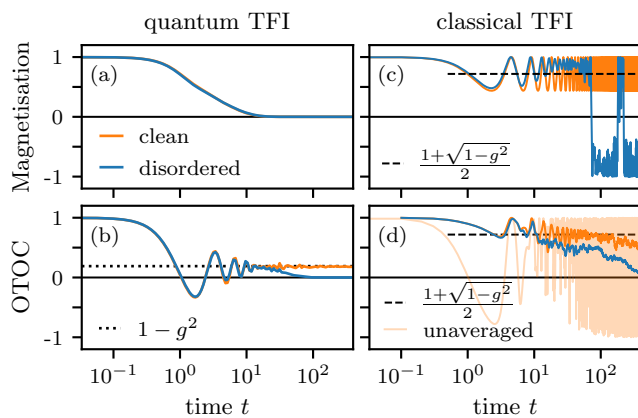


FIG. 1. Magnetisation (top) and OTOC (bottom) for quantum (left) and classical (right) Ising chains, for  $N = 500$  spins, coupling strength  $g = 0.9$  and open boundary conditions. Static spatial disorder is added to the transverse field (Gaussian with standard deviation  $W = 0.04$ ). (d) shows results averaged over a time window of about  $0.03t$  and over the nine sites closest to the perturbation to reduce fluctuations. For the classical simulations beyond  $t \gtrsim 50$ , the time evolution of the OTOC appears chaotic.

in contrast to the autocorrelator of the magnetisation. Subsequently, we illustrate how the underlying physical mechanisms—dynamical domain wall relocalisation alongside delocalisation—arise. The role of non-ergodicity is underlined by a discussion of the classical transverse field chain, and we conclude with a discussion of non-integrable systems.

*Model and observables.*— We study a chain of  $N$  spins- $1/2$  (represented by Pauli matrices  $\sigma_j^{x/y/z}$ ),

$$H_{\text{TFI}} = -J \sum_{j=1}^{N-1} \sigma_j^z \sigma_{j+1}^z + g \sum_{j=1}^N \sigma_j^x, \quad (1)$$

by mapping it to a non-interacting model of fermions corresponding to a  $p$ -wave superconductor [44, 45]. The model has Ising symmetry (generated by  $\mathcal{S} = \prod_{i=1}^N \sigma_i^x$ ) which is spontaneously broken for  $J > g$ , via a quantum phase transition at  $J = g$ . We monitor the magnetisation dynamics starting from an initial state  $|\Psi\rangle$ ,

$$M_{\Psi}(t) = \langle \Psi | e^{iHt} \sigma^z e^{-iHt} | \Psi \rangle. \quad (2)$$

In the thermodynamic limit (TDL), ordering in the (symmetry broken) groundstate  $|0\rangle$  is diagnosed by a non-zero  $M_0(t)$ .

In addition, for a quench starting with the fully polarised state, a simple OTOC consisting only of tensor product operators  $O_m, O_p$  of Pauli matrices  $\sigma^z$  has been proposed to act as a diagnostic of the phase transition [36, 37]:

$$C_{O_m, O_p}(t) = \langle \uparrow^N | [O_m, O_p(t)]^2 | \uparrow^N \rangle, \quad (3)$$

$n_p$	$n_m$	reloc. part	deloc. part	OTOC signal
even	even	1	1	1
even	odd	1	$\sqrt{1-g^2}^{n_p}$	$\sqrt{1-g^2}^{n_p}$
odd	even	$\sqrt{1-g^2}^{n_m}$	1	$\sqrt{1-g^2}^{n_m}$
odd	odd	$\sqrt{1-g^2}^{n_m}$	$\sqrt{1-g^2}^{n_p}$	$\sqrt{1-g^2}^{n_p+n_m}$

TABLE I. Late-time signals for the different OTOCs in the TDL for  $|g| \leq 1$ :  $\langle \uparrow^N | O_p(t) O_m O_p(t) | \uparrow^N \rangle$ , with  $O_p$  ( $O_m$ ) consisting of a product of  $n_p$  ( $n_m$ ) Pauli operators, for concreteness  $\sigma_{i_1}^z \sigma_{i_2}^z \dots \sigma_{i_n}^z$  at sites  $N/2, N/2+10, \dots, N/2+10(n-1)$ , with  $n \geq 1$ , so that the spatial support does not depend on system size. The superscript denotes whether the number is restricted to be even ( $e$ , excluding 0) or odd ( $o$ ). Note that an odd value of  $n_p$  leads to a dependence of the OTOC on  $n_m$ , and vice versa. A real space picture of the corresponding time evolution is given in Fig. 2 for the top pair of rows, and in the Appendix for the bottom pair.

with  $O_p(t) = e^{iHt} O_p e^{-iHt}$ . Note that  $\sigma_j^\alpha(t)$  being hermitian and unitary implies

$$C_{O_m, O_p}(t) = 2 \langle \uparrow^N | O_m O_p(t) O_m O_p(t) | \uparrow^N \rangle - 2 \quad (4)$$

The OTOC we consider is the non-trivial part  $\mathcal{F}(t) = \langle \uparrow^N | O_m O_p(t) O_m O_p(t) | \uparrow^N \rangle$  of  $C_{O_m, O_p}(t)$ . We refer to  $O_m$  as measured operator following the action of a perturbing operator  $O_p$ .

*Phenomenology in the transverse field Ising model.*— Our first central result consists of the time-dependent expectation values of the magnetisation and various OTOCs in the TDL, see Fig. 1 (a,b). This uses the analytical solution of the TFIM and Wick’s theorem as outlined in [46–49], with the late-time values of the OTOCs listed in Tab. I.

While  $M_0(t) \simeq (1 - \min(g, 1))^{1/8}$  [44],  $M_{\uparrow^N}(t) = 0$  at late times, see Fig. 1, as expected for a state with finite energy density [48–52]. By contrast, and as noted by [36], the OTOCs do mimic an order parameter, in that they are nonzero for  $g < J$  and vanishing otherwise. Note that these are evidently non-thermal: OTOCs which are Ising-even, such as those of the bond energy, should not vanish for  $g > J$ .

*A Domain Wall Perspective* In a standard picture, the vanishing of  $M_{\uparrow^N}$  arises due to freely propagating domain walls at finite density [52, 53]. This perspective can usefully be extended to explaining the behaviour of the OTOC. Technically, the TFIM allows for an exact solution as well as an elegant and physically transparent formulation of the Hamiltonian in terms of domain wall operators  $\tau_{j'}^x$  and  $\tau_{j'}^z \tau_{j'+1}^z$  acting on the dual lattice  $j' \in [1/2, N - 1/2]$ . Conceptually (and pictorially), for  $O_p$  consisting of  $\sigma^z$  operators, one can encode the domain wall dynamics by following the (out-of-time) evolution via a “BCS” pairing function  $X_{j'l'}$

$$U_{-t_b} O_p U_{t_f} | \uparrow^N \rangle \propto \prod_{j'l'} \left( 1 + X_{j'l'}(t_f, t_b) c_{j'}^\dagger c_{l'}^\dagger \right) | \uparrow^N \rangle \quad (5)$$

in terms of fermionic domain wall creation/annihilation operators with  $U_t = \exp(-iHt)$ , see App. B, extending

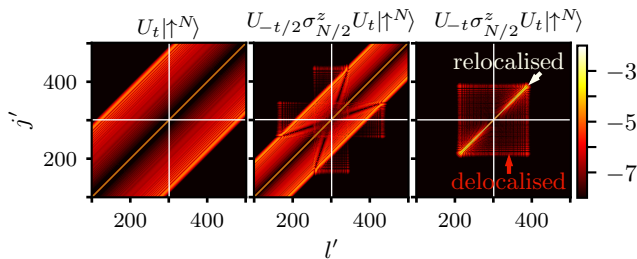


FIG. 2. Domain wall pairing, encoded by  $\log |X_{j'l'}|$  (Eq. (5)), for three different stages of the OTOC protocol: after the forward evolution to time  $t$ , as well during and after the back evolution. For the simulation we used  $N = 600, t = 300, J = 1, g = 0.3$  and show the bulk effects by setting  $100 \leq j', l' < 500$ .

[54]. In this formulation, the operators  $c_{j'}^\dagger c_{l'}^\dagger$  flip all spins between  $j'$  and  $l'$  if applied to the fully polarized state, e.g.

$$c_{j'}^\dagger c_{l'}^\dagger |\uparrow_1 \cdots \uparrow_N\rangle = |\uparrow_1 \cdots \uparrow_{j'-1} \downarrow_{j'} \cdots \downarrow_{l'-1} \uparrow_{l'} \cdots\rangle. \quad (6)$$

Our discussion is based on the snapshots of  $X_{j'l'}$  in Fig. 2:  $X_{j'l'}(t, 0)$  after a single forward time evolution (left), after half of the back evolution  $X_{j'l'}(t, t/2)$  (center) and after full back evolution  $X_{j'l'}(t, t)$  (right). The initial state  $|\uparrow^N\rangle$  has no domain walls. The domain walls, created in pairs, spread essentially independently, either in the same direction, so that  $X_{j'l'}(t, 0)$  close to the diagonal is nonzero or in opposite directions, yielding a wave front where  $X_{j'l'}(t, 0)$  is nonzero for  $|j' - l'| \approx 2v_{\text{wf}}t$  with the wavefront velocity  $v_{\text{wf}}$ , see Fig. 3. The following perturbation  $\sigma_j^z$  flips all signs  $\sigma_j^z c_{l'}^\dagger \sigma_j^z = \text{sign}(l' - j) c_{l'}^\dagger$  [55].

The late-time OTOC signal can then be assigned to arise from two mechanisms, which we term relocalisation and delocalisation.

Relocalisation is the (imperfect) back evolution of domain walls within the region  $2v_{\text{wf}}t$ , yielding large values for  $|X_{j'l'}(t, t)|$  close to the diagonal  $j' = l'$ , decaying exponentially with  $|j' - l'|$ .

The delocalisation mechanism is a perturbation of all ‘wave fronts’ close to the site of the perturbation  $\sigma_{N/2}^z$  yielding additional pairs of delocalised domain walls in  $\sigma_{N/2}^z(t) |\uparrow^N\rangle$ .

These mechanisms manifest themselves in the results summarised in in Tab. I as follows. Relocalisation is only effective in lowering the OTOC signal for odd  $n_p$ , as otherwise,  $O_p = \sigma_z^{\otimes n_p}$  commutes with the domain wall operators, Eq. (6), far away from the perturbation. For odd  $n_p$ , perturbed domain walls are relocalised within  $2v_{\text{wf}}t$  of the perturbation. The result of relocalisation alone is an only locally perturbed and, hence, globally low entangled state. Measuring this with  $n_m$  of  $\sigma^z$ s in  $O_m$  yields  $\approx \alpha^{n_m}$  where  $\alpha$  is the expectation value of a single  $\sigma^z$  operator in the relevant state. We derive analytically

$\alpha = \sqrt{1 - g^2}$  below.

Delocalisation, in turn, is invisible when  $n_m$  is even, as then,  $O_m$  commutes with the delocalized domain walls in the limit of late times. As each of the  $n_p$   $\sigma^z$ 's yields delocalized domain walls, for  $n_m$  odd, the measurement result is reduced by  $\beta^{n_p}$ , with  $\beta = \sqrt{1 - g^2}$  from numerics.

The re- and delocalisation mechanisms can be made transparent via an approximate calculation, as follows (for details, see App. C). The basic physical picture concerns the action of  $\sigma^z$  on a domain wall wavepacket with momentum components  $k'$  and concomitant group velocity  $v_g(k')$ . At large times, the components of the wavepacket with  $v_g > 0$  ( $v_g < 0$ ) will have moved a long way to the right (left) from the point of origin of the wavepacket at time  $t = 0$ . If  $\sigma^z$  acts in the region between,  $|x| \ll v_g t$ , its effect is to multiply each momentum components of the wavepacket with sign  $v_g = \text{sign } k'$ . Keeping this as the leading effect of  $\sigma^z$  then yields

$$X_{j'l'}^r(t) = -\text{sign}(j' - l') p^{-|j' - l'|} / 2 \quad (7)$$

with  $p = -g^{-1} - \sqrt{g^{-2} - 1}$  for  $|j' - l'| > 0$  and  $X_{j'l'} = 0$ : this is the exponential domain wall pair relocalisation, Fig. 3 (a). Plugging this form into Eq. (5) then yields the product state of rotated spins  $|\nearrow\rangle = \exp(i\gamma\sigma^y/2)|\uparrow\rangle$ ,  $\cos(\gamma) = 1 - g^2$  in which the polarisation  $\langle\sigma^z\rangle$  and domain wall density  $\langle c_i^\dagger c_i \rangle$  are straightforwardly related as  $\langle\sigma^z\rangle^2 = 1 - 2\langle c_i^\dagger c_i \rangle$ .

This also elegantly provides a handle on the delocalised part, which can be identified here as the difference between the exact result and our approximation:  $X^d = X - X^r$  is largely featureless and spreads out linearly with time as shown in Fig. 3.

Further down, in the discussion of integrability (see Fig. 4), we discuss the time-averaged domain wall density in the state  $|\uparrow^N(t)\rangle$ . Here we note that this is half as large as the value evaluated in the product state  $|\nearrow^N\rangle$ ,  $g^2/2$  ( $1/2$  for  $g > 1$ ) for the TFIM. This happens because the momentum modes in  $|\nearrow^N\rangle$  are permanently tilted with amplitudes between 0 and  $g^2$ , while they oscillate with the same amplitudes in  $|\uparrow^N(t)\rangle$ , see App. F.

*Classical Ising chain.* – Given the low entanglement of the effectively rotated state  $\sigma^z(t) |\uparrow^N\rangle$ , it is natural to consider an entirely classical version of the Ising chain, where we will find the role of dynamical constraints imposed by integrability and symmetry on the observables to be particularly transparent. Here, the vector of Pauli matrices is replaced by unit vectors  $\vec{S}_j$  undergoing precessional dynamics in their net (exchange+applied) field [56, 57]:

$$H = -J \sum_j S_j^z S_{j+1}^z + h \sum_j S_j^x. \quad (8)$$

Due to translational invariance of the initial (fully polarised) state, the equation of motion of  $M(t)$  – i.e., the zero-wavevector component of the magnetisation – decouples from the other momentum modes and effectively

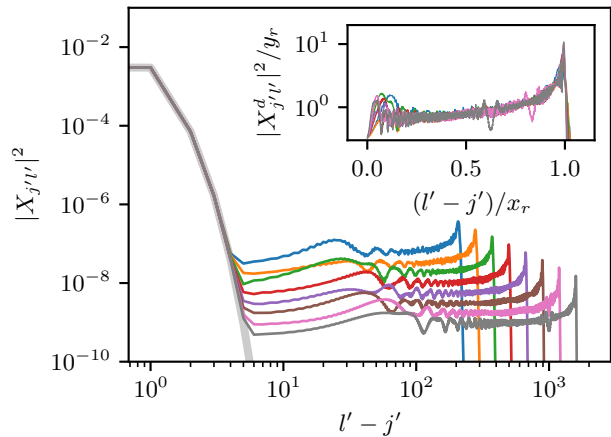


FIG. 3. Central row of  $|X_{j'l'}|^2$ , with parameters as in Fig. 2 but for larger systems  $N = 4000$  and times  $700 < t < 5300$ . The wide gray line indicates the exponential decay due to the relocalised domain wall pairs,  $X^r$  (Eq. (7)). The inset shows its deviation,  $|X_{j'l'}^d|^2 = |X_{j'l'} - X_{j'l'}^r|^2$ ; these curves collapse upon rescaling the axes with  $x_r = v_{wf}t \approx 0.3t$  and  $y_r = 0.04/t^2$ , respectively. The data is averaged over ten adjacent  $j'$  and two  $l'$ .

yields a single-spin problem. The resulting time evolution of  $M$  is fully periodic, Fig. 1 (c). Numerically, we find the functional form  $\sqrt{1 - g^2}$  for the amplitude of the periodic motion of the  $S^z$  component.

For the OTOC, the prescription for the classical counterpart to the OTOC is to forward evolve the fully polarised state, rotating the spin at site  $j$  by  $\pi$  around the  $z$ -axis and back evolving the state. By contrast to  $M(t)$ , this operation is no longer spatially uniform, but the state still remains polarised with a similar value as  $M(t)$ , at least for a long initial time, see Fig. 1(d).

*Role of integrability and disorder.*— The stability of  $M(t)$  for the classical case suggests that dynamical constraints – in this case the decoupling of the uniform  $k = 0$  mode of the spin density – plays a central role in the appearance of non-thermal late-time expectation values. To test this, we remove this decoupling by adding to the transverse field Gaussian white disorder with standard deviation  $W$ . This preserves the Ising symmetry of the system, while the uniformly polarised starting state also remains unchanged.

In the presence of already a small amount of disorder, the classical late-time signal in both  $M(t)$  and the OTOC vanishes, Fig. 1.

In the quantum system, it is the integrability of the TFIM which yields the (non-generic) conserved quantities, which follow from the decomposition of the system into  $2 \times 2$  blocks labelled by the momentum. The difficulty in confirming that these stabilise the OTOC signal lies in the fact that adding a generic perturbation removes integrability and hence makes the system intractable beyond small finite sizes.

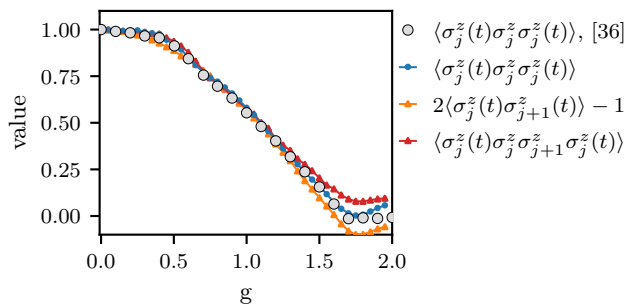


FIG. 4. Time-averaged correlators in the non-integrable ANNNI model: time-averaged OTOC (circles, from Ref. [36] and our own numerics), compared to domain wall density observables (triangles) evaluated in  $|\uparrow^N\rangle$  and  $|\sigma_j^z(t)\uparrow^N\rangle$ . The window for time averaging was chosen after initial transients (by eye), up to the time where boundary effects (determined by comparing  $N = 22$  and  $N = 24$  results) become visible. The data is most reliable for intermediate values of  $g \approx 1$ : for small  $g$  no clear plateau in the OTOC appears up to  $t = 120$ , while for large  $g$ , boundary effects set in early.

However, adding disorder to the transverse field keeps the single-particle nature of the problem intact while removing the dynamical constraints imposed by translational symmetry and the concomitant momentum conservation. Indeed, doing so immediately degrades the signal of the OTOC, Fig. 1 (b), indicating that indeed, the dynamical constraints underpin the late-time signal.[58]

*Fate of the OTOC beyond integrability.*— Based on general considerations about chaos and the butterfly effect, one would expect late-time observables inside the lightcone (Fig. 2) to take on the values characteristic of the energy density of the fully polarised state from which the quench started—these values are zero for both magnetisation and OTOC. However, for the TFIM this is patently not the case. Concretely, even a local observable such as the exchange energy of neighbouring spins,  $J \sigma_j^z \sigma_{j+1}^z$  takes on a non-thermal value, namely it vanishes for  $g > 1$ .

One might therefore be tempted to propose  $J \sigma_j^z \sigma_{j+1}^z$  as a diagnostic for the phase transition, alongside the OTOC. However, it seems to us that a converse line of argument is more compelling: both features are due to the dynamical constraints imposed by integrability. Given the small system sizes accessible for non-integrable models, what is observed there is then a prethermal expectation value, i.e. a vestige of the integrable signal because the scattering processes between domain walls are not sufficient for degrading the signal before finite-size effects mask the behaviour of the thermodynamic system. This conclusion is also supported by the fact that removing the dynamical constraints only partially via the disordered transverse field already degrades the signal considerably.

In fact, we note that the ANNNI model studied in Ref. [36, 49, 59], where a second-neighbour interaction is added that breaks integrability,  $H_{\text{ANNNI}} = H_{\text{TFI}} - \Delta \sum_{j=1}^{N-2} \sigma_j^z \sigma_{j+2}^z$ , is close to integrable in two ways. First,

due to the smallness of  $\Delta$ , the integrability-breaking perturbation itself. Second, a four-fermion term of the form

$$H_{\text{int}} \sim -4\Delta \sum_i c_{j'}^\dagger c_{j'} c_{j'+1}^\dagger c_{j'+1}. \quad (9)$$

appears. This is separately small due to the diluteness of quasiparticles, with the domain wall density  $c_{j'}^\dagger c_{j'} \sim g^2/4$ . Intriguingly, we find that the correspondence between domain wall density and the OTOC identified for the TFIM persists for the ANNNI model at the accessible times, see Fig. 4. While a controlled theory for the case where neither  $\Delta$  nor  $g$  are small would clearly be desirable, it seems to us that there appears to be no need to invoke absence/presence of order to explain the behaviour of the OTOC.

*Conclusion.*— Via a combined numerical and analytical study of an OTOC in an Ising chain, we have analysed the interplay of order with many-body dynamics, thermalisation and integrability. For the integrable case, where we have identified the mechanism, dynamical do-

main wall relocalisation, underpinning the persistent signal, our treatment is fairly comprehensive; much work remains to be done to fully understand the behaviour of generic many-body systems, here and in higher dimension.

## ACKNOWLEDGMENTS

We are grateful to Fabian Essler, Markus Heyl, Dima Kovrizhin, Adam McRoberts, Benedikt Placke, Frank Pollmann and Jonathan Nilsson Hallén for engaging discussions. This work was in part supported by the Deutsche Forschungsgemeinschaft under grants SFB 1143 (project-id 247310070) and the cluster of excellence ct.qmat (EXC 2147, project-id 390858490). V.K. was supported in part by the US Department of Energy, Office of Science, Basic Energy Sciences, under Early Career Award No. DE-SC0021111. V.K. also acknowledges support from the Sloan Foundation through a Sloan Research Fellowship and the Packard Foundation through a Packard Fellowship.

- 
- [1] I. Bloch, J. Dalibard, and W. Zwerger, Many-body physics with ultracold gases, *Rev. Mod. Phys.* **80**, 885 (2008).
- [2] I. Bloch, J. Dalibard, and S. Nascimbene, Quantum simulations with ultracold quantum gases, *Nature Physics* **8**, 267 (2012).
- [3] R. Blatt and C. F. Roos, Quantum simulations with trapped ions, *Nature Physics* **8**, 277 (2012).
- [4] I. M. Georgescu, S. Ashhab, and F. Nori, Quantum simulation, *Rev. Mod. Phys.* **86**, 153 (2014).
- [5] M. Schreiber, S. S. Hodgman, P. Bordia, H. P. Lüschen, M. H. Fischer, R. Vosk, E. Altman, U. Schneider, and I. Bloch, Observation of many-body localization of interacting fermions in a quasirandom optical lattice, *Science* **349**, 842 (2015).
- [6] J. Smith, A. Lee, P. Richerme, B. Neyenhuis, P. W. Hess, P. Hauke, M. Heyl, D. A. Huse, and C. Monroe, Many-body localization in a quantum simulator with programmable random disorder, *Nature Physics* **12**, 907 (2016).
- [7] P. Bordia, H. P. Lüschen, S. S. Hodgman, M. Schreiber, I. Bloch, and U. Schneider, Coupling identical one-dimensional many-body localized systems, *Physical Review Letters* **116**, 10.1103/physrevlett.116.140401 (2016).
- [8] J. yoon Choi, S. Hild, J. Zeiher, P. Schauß, A. Rubio-Abadal, T. Yefsah, V. Khemani, D. A. Huse, I. Bloch, and C. Gross, Exploring the many-body localization transition in two dimensions, *Science* **352**, 1547 (2016), <https://www.science.org/doi/pdf/10.1126/science.aaf8834>.
- [9] E. A. Martinez, C. A. Muschik, P. Schindler, D. Nigg, A. Erhard, M. Heyl, P. Hauke, M. Dalmonte, T. Monz, P. Zoller, and R. Blatt, Real-time dynamics of lattice gauge theories with a few-qubit quantum computer, *Nature* **534**, 516 (2016).
- [10] N. Fläschner, D. Vogel, M. Tarnowski, B. S. Rem, D. S. Lühmann, M. Heyl, J. C. Budich, L. Mathey, K. Sengstock, and C. Weitenberg, Observation of dynamical vortices after quenches in a system with topology, *Nature Physics* **14**, 265 (2018).
- [11] P. Jurcevic, H. Shen, P. Hauke, C. Maier, T. Brydges, C. Hempel, B. Lanyon, M. Heyl, R. Blatt, and C. Roos, Direct observation of dynamical quantum phase transitions in an interacting many-body system, *Physical Review Letters* **119**, 10.1103/physrevlett.119.080501 (2017).
- [12] J. Zhang, G. Pagano, P. W. Hess, A. Kyprianidis, P. Becker, H. Kaplan, A. V. Gorshkov, Z. X. Gong, and C. Monroe, Observation of a many-body dynamical phase transition with a 53-qubit quantum simulator, *Nature* **551**, 601 (2017).
- [13] J. Zhang, P. W. Hess, A. Kyprianidis, P. Becker, A. Lee, J. Smith, G. Pagano, I.-D. Potirniche, A. C. Potter, A. Vishwanath, N. Y. Yao, and C. Monroe, Observation of a discrete time crystal, *Nature* **543**, 217 (2017).
- [14] S. Choi, J. Choi, R. Landig, G. Kucsko, H. Zhou, J. Isoya, F. Jelezko, S. Onoda, H. Sumiya, V. Khemani, C. von Keyserlingk, N. Y. Yao, E. Demler, and M. D. Lukin, Observation of discrete time-crystalline order in a disordered dipolar many-body system, *Nature* **543**, 221 (2017).
- [15] M. K. Joshi, A. Elben, B. Vermersch, T. Brydges, C. Maier, P. Zoller, R. Blatt, and C. F. Roos, Quantum information scrambling in a trapped-ion quantum simulator with tunable range interactions, *Phys. Rev. Lett.* **124**, 240505 (2020).
- [16] R. J. Lewis-Swan, A. Safavi-Naini, A. M. Kaufman, and A. M. Rey, Dynamics of quantum information, *Nature Reviews Physics* **1**, 627 (2019).
- [17] Z. Lenarčič, F. Lange, and A. Rosch, Perturbative approach to weakly driven many-particle systems in the

- presence of approximate conservation laws, *Physical Review B* **97**, [10.1103/physrevb.97.024302](https://doi.org/10.1103/physrevb.97.024302) (2018).
- [18] A. I. Larkin and Y. N. Ovchinnikov, Quasiclassical Method in the Theory of Superconductivity, *Soviet Journal of Experimental and Theoretical Physics* **28**, 1200 (1969).
- [19] J. Li, R. Fan, H. Wang, B. Ye, B. Zeng, H. Zhai, X. Peng, and J. Du, Measuring out-of-time-order correlators on a nuclear magnetic resonance quantum simulator, *Phys. Rev. X* **7**, [031011](https://doi.org/10.1103/physrevx.7.031011) (2017).
- [20] M. Gärttner, J. G. Bohnet, A. Safavi-Naini, M. L. Wall, J. J. Bollinger, and A. M. Rey, Measuring out-of-time-order correlations and multiple quantum spectra in a trapped-ion quantum magnet, *Nature Physics* **13**, 781 (2017).
- [21] N. Y. Yao, F. Grusdt, B. Swingle, M. D. Lukin, D. M. Stamper-Kurn, J. E. Moore, and E. A. Demler, *Interferometric approach to probing fast scrambling* (2016).
- [22] B. Swingle, G. Bentsen, M. Schleier-Smith, and P. Hayden, Measuring the scrambling of quantum information, *Physical Review A* **94**, [10.1103/physreva.94.040302](https://doi.org/10.1103/physreva.94.040302) (2016).
- [23] G. Zhu, M. Hafezi, and T. Grover, Measurement of many-body chaos using a quantum clock, *Physical Review A* **94**, [10.1103/physreva.94.062329](https://doi.org/10.1103/physreva.94.062329) (2016).
- [24] M. Campisi and J. Goold, Thermodynamics of quantum information scrambling, *Physical Review E* **95**, [10.1103/physreve.95.062127](https://doi.org/10.1103/physreve.95.062127) (2017).
- [25] I. L. Aleiner, L. Faoro, and L. B. Ioffe, Microscopic model of quantum butterfly effect: Out-of-time-order correlators and traveling combustion waves, *Annals of Physics* **375**, 378 (2016).
- [26] A. Bohrdt, C. B. Mendl, M. Endres, and M. Knap, Scrambling and thermalization in a diffusive quantum many-body system, *New Journal of Physics* **19**, 063001 (2017).
- [27] R. Fan, P. Zhang, H. Shen, and H. Zhai, Out-of-time-order correlation for many-body localization, *Science Bulletin* **62**, 707 (2017).
- [28] Y. Huang, Y.-L. Zhang, and X. Chen, Out-of-time-ordered correlators in many-body localized systems, *Annalen der Physik* **529**, 1600318 (2016).
- [29] J. Maldacena, S. H. Shenker, and D. Stanford, A bound on chaos, *Journal of High Energy Physics* **2016**, [10.1007/jhep08\(2016\)106](https://doi.org/10.1007/jhep08(2016)106) (2016).
- [30] P. Hayden and J. Preskill, Black holes as mirrors: quantum information in random subsystems, *Journal of High Energy Physics* **2007**, 120 (2007).
- [31] Y. Sekino and L. Susskind, Fast scramblers, *Journal of High Energy Physics* **2008**, 065 (2008).
- [32] C. von Keyserlingk, T. Rakovszky, F. Pollmann, and S. Sondhi, Operator hydrodynamics, OTOCs, and entanglement growth in systems without conservation laws, *Physical Review X* **8**, [10.1103/physrevx.8.021013](https://doi.org/10.1103/physrevx.8.021013) (2018).
- [33] V. Khemani, A. Vishwanath, and D. A. Huse, Operator spreading and the emergence of dissipative hydrodynamics under unitary evolution with conservation laws, *Phys. Rev. X* **8**, [031057](https://doi.org/10.1103/physrevx.8.031057) (2018).
- [34] T. Rakovszky, F. Pollmann, and C. von Keyserlingk, Diffusive hydrodynamics of out-of-time-ordered correlators with charge conservation, *Physical Review X* **8**, [10.1103/physrevx.8.031058](https://doi.org/10.1103/physrevx.8.031058) (2018).
- [35] S. Zamani, R. Jafari, and A. Langari, Out-of-time-order correlations and floquet dynamical quantum phase transition, *Phys. Rev. B* **105**, 094304 (2022).
- [36] M. Heyl, F. Pollmann, and B. Dóra, Detecting equilibrium and dynamical quantum phase transitions in ising chains via out-of-time-ordered correlators, *Physical Review Letters* **121**, [10.1103/physrevlett.121.016801](https://doi.org/10.1103/physrevlett.121.016801) (2018).
- [37] C. B. Dağ, K. Sun, and L.-M. Duan, Detection of quantum phases via out-of-time-order correlators, *Physical Review Letters* **123**, [10.1103/physrevlett.123.140602](https://doi.org/10.1103/physrevlett.123.140602) (2019).
- [38] Q. Wang and F. Pérez-Bernal, Probing an excited-state quantum phase transition in a quantum many-body system via an out-of-time-order correlator, *Phys. Rev. A* **100**, 062113 (2019).
- [39] Z.-H. Sun, J.-Q. Cai, Q.-C. Tang, Y. Hu, and H. Fan, Out-of-time-order correlators and quantum phase transitions in the rabi and dicke models, *Annalen der Physik* **532**, 1900270 (2020).
- [40] H. Shen, P. Zhang, R. Fan, and H. Zhai, Out-of-time-order correlation at a quantum phase transition, *Phys. Rev. B* **96**, 054503 (2017).
- [41] X. Nie, B.-B. Wei, X. Chen, Z. Zhang, X. Zhao, C. Qiu, Y. Tian, Y. Ji, T. Xin, D. Lu, and J. Li, Experimental observation of equilibrium and dynamical quantum phase transitions via out-of-time-ordered correlators, *Phys. Rev. Lett.* **124**, 250601 (2020).
- [42] B. Chen, X. Hou, F. Zhou, P. Qian, H. Shen, and N. Xu, Detecting the out-of-time-order correlations of dynamical quantum phase transitions in a solid-state quantum simulator, *Applied Physics Letters* **116**, 194002 (2020).
- [43] P. Titum, J. T. Iosue, J. R. Garrison, A. V. Gorshkov, and Z.-X. Gong, Probing ground-state phase transitions through quench dynamics, *Phys. Rev. Lett.* **123**, 115701 (2019).
- [44] P. Pfeuty, The one-dimensional ising model with a transverse field, *Annals of Physics* **57**, 79 (1970).
- [45] M. Sigrist, Introduction to unconventional superconductivity (2005).
- [46] E. Lieb, T. Schultz, and D. Mattis, Two soluble models of an antiferromagnetic chain, *Annals of Physics* **16**, 407 (1961).
- [47] C.-J. Lin and O. I. Motrunich, Out-of-time-ordered correlators in a quantum ising chain, *Physical Review B* **97**, [10.1103/physrevb.97.144304](https://doi.org/10.1103/physrevb.97.144304) (2018).
- [48] P. Calabrese, F. H. L. Essler, and M. Fagotti, Quantum quench in the transverse field ising chain: I. time evolution of order parameter correlators, *Journal of Statistical Mechanics: Theory and Experiment* **2012**, P07016 (2012).
- [49] D. Rossini, S. Suzuki, G. Mussardo, G. E. Santoro, and A. Silva, Long time dynamics following a quench in an integrable quantum spin chain: Local versus nonlocal operators and effective thermal behavior, *Physical Review B* **82**, [10.1103/physrevb.82.144302](https://doi.org/10.1103/physrevb.82.144302) (2010).
- [50] M. Heyl, A. Polkovnikov, and S. Kehrein, Dynamical quantum phase transitions in the transverse-field ising model, *Physical Review Letters* **110**, [10.1103/physrevlett.110.135704](https://doi.org/10.1103/physrevlett.110.135704) (2013).
- [51] M. Fagotti and F. H. L. Essler, Reduced density matrix after a quantum quench, *Physical Review B* **87**, [10.1103/physrevb.87.245107](https://doi.org/10.1103/physrevb.87.245107) (2013).
- [52] F. H. L. Essler and M. Fagotti, Quench dynamics and relaxation in isolated integrable quantum spin chains, *Journal of Statistical Mechanics: Theory and Experiment*

- ment **2016**, 064002 (2016).
- [53] H. Rieger and F. Iglói, Semiclassical theory for quantum quenches in finite transverse ising chains, *Physical Review B* **84**, [10.1103/physrevb.84.165117](#) (2011).
- [54] G. B. Mbeng, A. Russomanno, and G. E. Santoro, *The quantum ising chain for beginners* (2020), [arXiv:2009.09208 \[quant-ph\]](#).
- [55] Here we use open boundary conditions or a infinitely larger system, see App. A, E.
- [56] D. Schubert, J. Richter, F. Jin, K. Michielsen, H. De Raedt, and R. Steinigeweg, Quantum versus classical dynamics in spin models: Chains, ladders, and square lattices, *Physical Review B* **104**, [10.1103/physrevb.104.054415](#) (2021).
- [57] T. Bilitewski, S. Bhattacharjee, and R. Moessner, Classical many-body chaos with and without quasiparticles, *Physical Review B* **103**, [10.1103/physrevb.103.174302](#) (2021).
- [58] We note that, while the disorder reduces the dynamical relocalisation of domain walls, it instead leads to their Anderson localization, so that for stronger disorder with a short localisation length, the OTOC remains visibly nonzero.
- [59] C. Karrasch and D. Schuricht, Dynamical phase transitions after quenches in nonintegrable models, *Physical Review B* **87**, [10.1103/physrevb.87.195104](#) (2013).